

Electronic Supporting Information

“Structurally-neutral” densely packed homopolymer adsorbed chains for directed self-assembly of block copolymer thin films

Yuma Morimitsu^{1,2,‡}, Daniel Salatto^{1,‡}, Naisheng Jiang¹, Mani Sen¹, Shotaro Nishitsuji^{1,3}, Benjamin M. Yavitt¹, Maya K. Endoh¹, Ashwanth Subramanian¹, Chang-Yong Nam⁴, Ruipeng Li⁵, Masafumi Fukuto⁵, Yugang Zhang⁵, Lutz Wiegart⁵, Andrei Fluerasu⁵, Keiji Tanaka², Tadanori Koga^{1,6,*}

¹Department of Materials Science and Chemical Engineering, Stony Brook University, Stony Brook, New York 11794-2275

²Department of Applied Chemistry, Kyushu University, Fukuoka 819-0395, Japan

³Graduate School of Science and Engineering, Yamagata University, Yonezawa, Yamagata 992-8510, Japan

⁴Center for Functional Nanomaterials, Brookhaven National Laboratory, Upton, NY 11973-5000, USA

⁵National Synchrotron Light Source II, Brookhaven National Laboratory, Upton, New York 11973

⁶Department of Chemistry, Stony Brook University, Stony Brook, New York 11794-3400, Japan

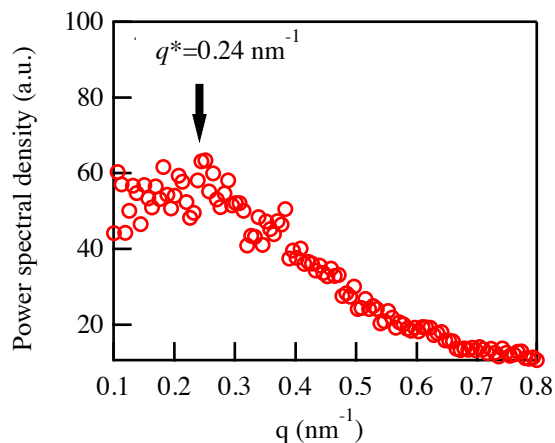


Figure S1. FFT of the AFM image shown in Fig. 2a. The broad peak corresponds to the average interdomain spacing of the distorted lamellar microdomains in the PS-*block*-PMMA interfacial sublayer. Note that the interdomain spacing estimated from the the peak position is slightly larger (~ 26 nm) than that in the bulk (20 nm), suggesting that the packing of the lamellar microdomain formed in the interfacial sublayer is poor.

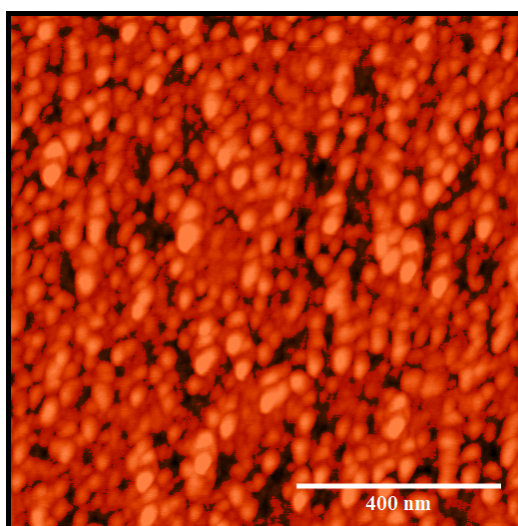


Figure S2. Representative surface coverage analysis for the PS50k nanocoating. The area occupied by the polymer above a critical threshold is colored in red (bearing area analysis using NanoScope Analysis software (version 1.40, Bruker). The detail has been described elsewhere¹. The total surface coverage was estimated to be about 85%.

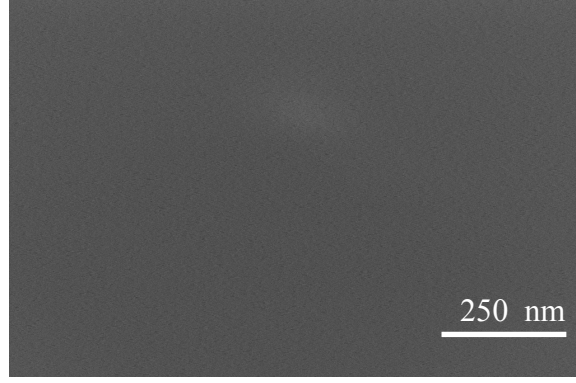


Figure S3. SEM image of the 60 nm-thick PS-*block*-PMMA film surface on the PS50k nanocoating annealed at 140 °C.

Effect of a rough surface. According to a theoretical study², the transition in BCP domains (lamella and cylinder) from parallel to perpendicular orientations on corrugated surfaces is induced when the difference between the two free energies on two different microdomain orientations meet the following relation:

$$F_{para} - F_{per} \propto \left(\frac{q_{BCP}}{q_{sub}} \right)^2 (q_{BCP}R)^2 - 1 > 0, \quad (1)$$

where F_{para} and F_{per} are the bulk free energy of the parallel and perpendicular orientations, respectively, $q_{BCP} \equiv 2\pi/L_0$ is the wavenumber of the microdomain spacing of a BCP, $q_{sub} \equiv 2\pi/\lambda_r$ is the wavenumber of the lateral characteristic length (λ_r) of a rough substrate surface, and R is the root mean-square vertical displacement of the surface topography from a mean horizontal line. Hence, if q_{BCP} is fixed and R and q_{sub} vary, the perpendicular orientation is favored when $q_{BCP}R > q_{sub}/q_{BCP}$, while the parallel orientation is favored at $q_{BCP}R < q_{sub}/q_{BCP}$. It was postulated that for a sufficiently rough surface, the increase in the free energy through bending deformations of a parallel orientation is higher than the energy penalty for a perpendicular orientation on rough surfaces (i.e., the perpendicular orientation is favored even on a non-neutral surface). This concept was verified using nearly symmetric lamellar forming PS-*block*-PMMA on different non-neutral surfaces³⁻⁵.

Motivated by the above theoretical and experimental results, we examined the effect of the surface roughness of the PS50k nanocoating on the perpendicular microdomain formation. Based on the AFM image analysis (Figure S4), the $q_{sub}R$ values for the PS 50k flattened layer was estimated to be about 0.10 ± 0.02 . Therefore, this $q_{sub}R$ value is much smaller than the critical $q_{sub}/q_{BCP} \sim 0.42$ above which a perpendicular orientation of lamellar microdomains takes place for the same PS-*block*-PMMA ($M_{w,PS}=18,500$ g/mol, $M_{w,PMMA}=18,000$ g/mol) prepared on a rough substrate⁴. Hence, these results rule out the effect of the surface roughness on the resultant perpendicular microdomains orientation.

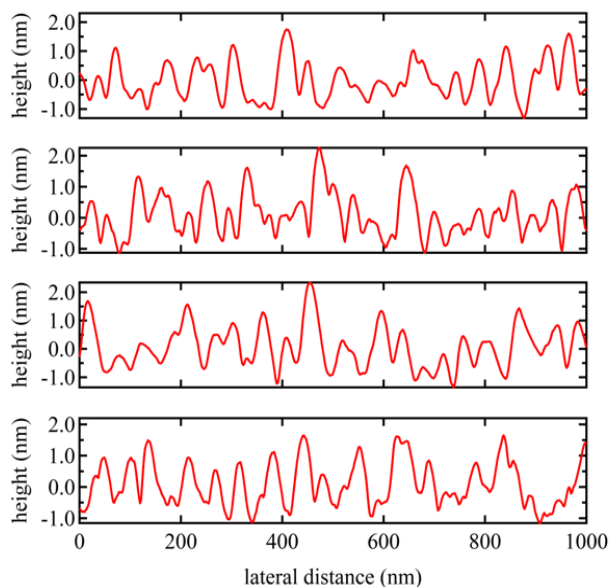


Figure S4. Representative cross-sectional profiles of the height image of PS50k flattened layer on the HF-etched Si substrate at four different cross sections. The averaged wavenumber of the lateral characteristic length (λ_r) and the root mean-square vertical displacement (R) values were estimated using Gwyddion 2.51 software from ten different cross-sectional profiles of the image.

PMMA nanocoating. We also prepared PMMA nanocoatings with different molecular weight ($M_n=44\text{kDa}$, $M_w/M_n=1.02$, Polymer Source, hereafter assigned as PMMA44k) and characterized them with X-ray reflectivity. Figure S5 shows the XR profile of the PMMA44k nanocoating at 25 °C. The thickness of the PMMA44k nanocoating was determined to be 3.2 nm, which is identical to that of the PMMA97k nanocoating. At the same time, we conducted similar experiments discussed in the main text to check whether the PMMA44k nanocoating prevents the growth of the loosely adsorbed PS-*block*-PMMA chains. We prepared a 60 nm-thick PS-*block*-PMMA thin film on top

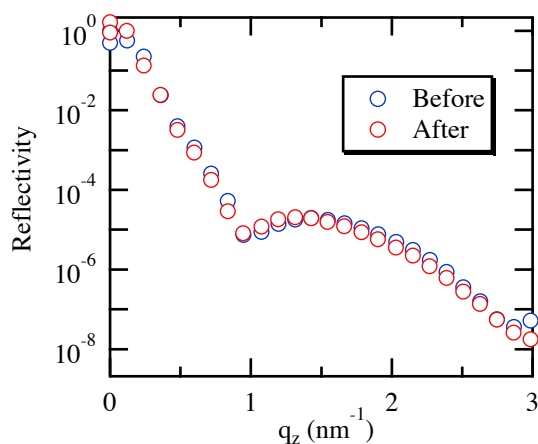


Figure S5 XR profiles of the PMMA44k nanocoating before and after the PS-*block*-PMMA adsorption test on the nanocoating. The error bars are within the sizes of the symbols.

of the PMMA44k nanocoating and thermally annealed it at 200 °C for 12h. The bilayer film was then solvent leached with toluene (a total of 3 cycles of leaching at room temperature with 5 min per each cycle) and subsequently dried at 200 °C under vacuum for overnight to remove any residual solvent molecules. Figure S5 also plots the XR result of the PMMA44k nanocoating after the adsorption experiment. Hence we can see that the XR profiles remain nearly unchanged before and after the adsorption test. Hence, it is reasonable to conclude that the PMMA nanocoating is also non-interactive with the PS and PMMA blocks, thereby acting as a “structurally neutral” surface coating.

References

1. Jiang, N.; Shang, J.; Di, X.; Endoh, M. K.; Koga, T. Formation Mechanism of High-Density, Flattened Polymer Nanolayers Adsorbed on Planar Solids, *Macromolecules* **2014**, 47, 2682-2689.
2. Tsori, Y.; Andelman, D. Parallel and Perpendicular Lamellae on Corrugated Surfaces, *Macromolecules* **2003**, 36, 8560-8566.
3. Sivaniah, E.; Hayashi, Y.; Iino, M.; Hashimoto, T.; Fukunaga, K. Observation of Perpendicular Orientation in Symmetric Diblock Copolymer Thin Films on Rough Substrates, *Macromolecules* **2003**, 36, 5894-5896.
4. Sivaniah, E.; Hayashi, Y.; Matsubara, S.; Kiyono, S.; Hashimoto, T.; Fukunaga, K.; Kramer, E. J.; Mates, T. Symmetric Diblock Copolymer Thin Films on Rough Substrates. Kinetics and Structure Formation in Pure Block Copolymer Thin Films, *Macromolecules* **2005**, 38, 1837-1849.
5. Kim, T.; Wooh, S.; Son, J. G.; Char, K. Orientation Control of Block Copolymer Thin Films Placed on Ordered Nanoparticle Monolayers, *Macromolecules* **2013**, 46, 8144-8151.